Physics Letters B 689 (2010) 172–176

Contents lists available at ScienceDirect

Physics Letters B

www.elsevier.com/locate/physletb

Resonant production of color octet electron at the LHeC

M. Sahin [a,*], S. Sultansoy [a,b], S. Turkoz [c]

[a] TOBB University of Economics and Technology, Physics Division, Ankara, Turkey
[b] Institute of Physics, National Academy of Sciences, Baku, Azerbaijan
[c] Ankara University, Department of Physics, Ankara, Turkey

ARTICLE INFO

Article history:
Received 27 January 2010
Received in revised form 7 April 2010
Accepted 28 April 2010
Editor: G.F. Giudice

Keywords:
ep collisions
LHeC
QCD Explorer
Preonic models
Leptogluon

ABSTRACT

In composite models with colored preons leptogluons (l_8) has a same status with leptoquarks, excited leptons and quarks, etc. We analyze resonant production of color octet electron (e_8) at QCD Explorer stage of the Large Hadron electron Collider (LHeC). It is shown that the e_8 discovery at the LHeC simultaneously will determine the compositeness scale.

1. Introduction

A large number of "fundamental" particles, as well as observable free parameters (put by hand), in Standard Model (SM) indicate that it is not "the end of story". Physics has met similar situation two times in the past: one was the Periodic Table of the Elements which was clarified by Rutherford's experiment later, the other was the hadron inflation which has resulted in quark model. This analogy implies the preonic structure of the SM fermions (see [1] and references therein). The preonic models predict a zoo of new particles such as excited leptons and quarks, leptoquarks, leptogluons, etc. Excited fermions and leptoquarks are widely discussed in literature and their searches are inseparable parts of future collider's physics programs. Unfortunately, leptogluons did not attract necessary attention, while they are predicted in all models with colored preons [2–7]. For example, in the framework of fermion-scalar models, leptons would be a bound state of one fermionic preon and one scalar anti-preon $l = (F\bar{S}) = 1 \oplus 8$ (both F and S are color triplets), then each SM lepton has its own color octet partner [7].

Lower bound on leptogluon masses, 86 GeV, given in PDG [8] reflects twenty years old Tevatron results [9]. As mentions in [10] D0 clearly exclude 200 GeV leptogluons and could naively place the constraint $M_{LG} \gtrsim 325$ GeV. The fifteen years old H1 data on color octet electron, e_8, search [11] has excluded the compositeness scale $\Lambda \lesssim 3$ TeV for $M_{e8} \backsimeq 100$ GeV and $\Lambda \lesssim 240$ GeV for $M_{e8} \backsimeq 250$ GeV. The advantage of lepton–hadron colliders is the resonant production of leptogluons, whereas at hadron and lepton colliders they are produced in pairs.

The sole realistic way to TeV scale in lepton–hadron collisions are presented by linac-ring type electron–proton colliders (see reviews [12–14] and references therein). Recently CERN, ECFA and NuPECC initiated the study on the LHC based ep colliders [15]. Two options are considered for the Large Hadron electron Collider (LHeC): the construction of new e-ring in the LHC tunnel [16] or the construction of e-linac tangentially to the LHC [17–19]. It should be noted that in first option the energy of electrons is limited by synchrotron radiation, whereas in second option the energy of electrons can be increased by lengthening the linac. Tentative parameters for linac-ring options of the LHeC are presented in Table 1. QCD Explorer stage(s) is mandatory: it will provide necessary information on PDF's for adequate interpretation of future LHC results and it will clarify QCD basics, as well. The realization of the Energy Frontier stage(s) will be determined by the LHC data on Beyond the Standard Model (BSM) physics.

In this Letter we investigate potential of QCDE stages of the LHeC in search for color octet electron via resonant production. In Section 2, Lagrangian for e_8 interactions is presented and it's decay widths and production cross sections at different stages of LHeC are evaluated. Section 3 is devoted to the analysis of leptogluon signatures at QCD-E stages of the LHeC. Finally, the concluding remarks are given in Section 4.

* Corresponding author.
E-mail addresses: m.sahin@etu.edu.tr (M. Sahin), ssultansoy@etu.edu.tr (S. Sultansoy), turkoz@science.ankara.edu.tr (S. Turkoz).

0370-2693
doi:10.1016/j.physletb.2010.04.070

Table 1
Tentative parameters of the LHeC linac-ring options. QCDE and EF denotes QCD Explorer and Energy Frontier, respectively.

Stage	E_e, GeV	$\sqrt{s}$, TeV	L, 10^{32} cm^{-2} s^{-1}
LHeC/QCDE-1	70	1.4	1–10
LHeC/QCDE-2	140	1.98	1–10
LHeC/EF	500	3.74	1

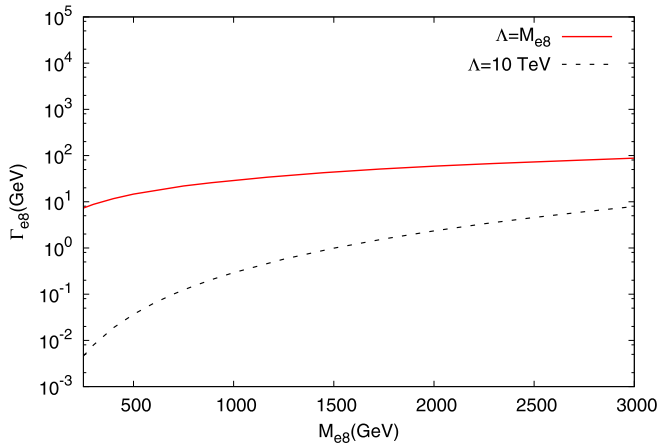

Fig. 1. Leptogluon decay width via its mass for $\Lambda = M_{e8}$ and $\Lambda = 10$ TeV.

2. Interaction Lagrangian, decay width and production cross section

For the interaction of leptogluons with the corresponding lepton and gluon we use the following Lagrangian [8,20]:

$$L = \frac{1}{2\Lambda}\sum_{l}\left\{\bar{l}_8^{\alpha} g_s G^{\alpha}_{\mu\nu}\sigma^{\mu\nu}(\eta_L l_L + \eta_R l_R) + \text{h.c.}\right\} \tag{1}$$

where $G^{\alpha}_{\mu\nu}$ is the field strength tensor for gluon, index $\alpha = 1, 2, \ldots, 8$ denotes the color, g_s is gauge coupling, η_L and η_R are the chirality factors, l_L and l_R denote left and right spinor components of lepton, $\sigma^{\mu\nu}$ is the anti-symmetric tensor and Λ is the compositeness scale. The leptonic chiral invariance implies $\eta_L\eta_R = 0$. For numerical calculations we add leptogluons into the CalcHEP program [21].

Decay width of the color octet electron is given by

$$\Gamma_{e8} = \frac{\alpha_s M_{e8}^3}{4\Lambda^2} \tag{2}$$

In Fig. 1 the decay widths of leptogluons are presented for two scenarios, $\Lambda = M_{e8}$ and $\Lambda = 10$ TeV.

The resonant e_8 production cross sections for the there stages of the LHeC from Table 1, evaluated using CalcHEP with CTEQ6L parametrization [22] for parton distribution functions, are presented in Figs. 2–4. It is seen that sufficiently high cross-section values allow the exploration of the e_8 mass range almost up to the kinematical limits.

3. Signal and background analysis

3.1. LHeC/QCDE-1 stage

First of all, let us consider p_T and η distributions for signal and background processes in order to determine appropriate kinematical cuts. All calculations were performed at the partonic level using CalcHEP simulation program [21] with CTEQ6L parton distributions functions [22]. Hereafter the term jet means gluon for

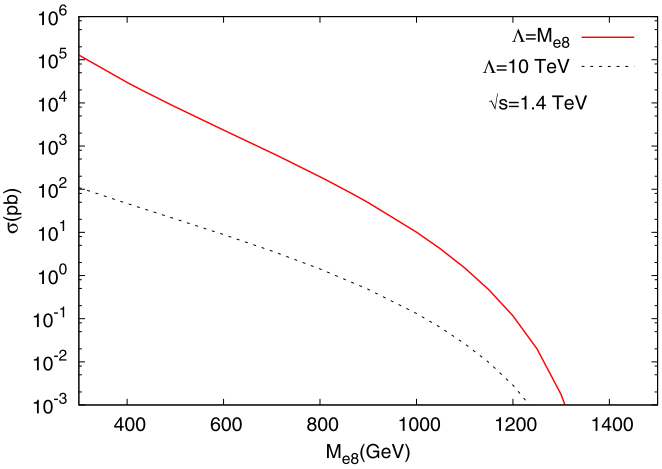

Fig. 2. Resonant e_8 production at the LHeC/QCDE-1.

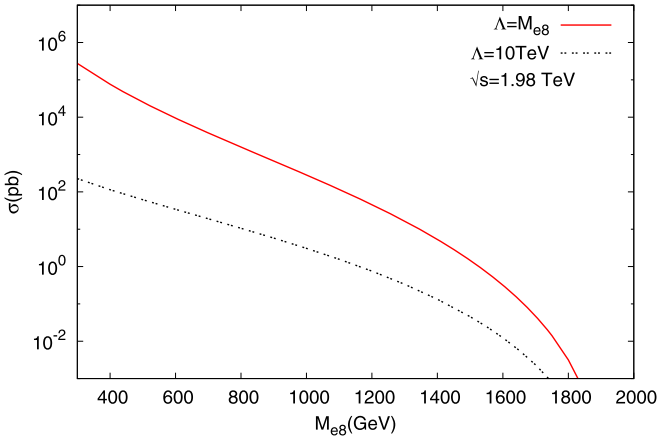

Fig. 3. Resonant e_8 production at the LHeC/QCDE-2.

signal and quarks (u, $\bar{u}$, d, $\bar{d}$, c, $\bar{c}$, s, $\bar{s}$, b, $\bar{b}$) for background processes. At the partonic level, the signal process is $e^-g \to e_8 \to e^-g$ and background processes are $e^-q \to e^-q$ (through γ and Z exchange), which give main contribution to the background. The other background processes: (i) $e^-q \to e^-W^-q$, (ii) $e^-q \to e^-qg$ and $e^-g \to e^-q\bar{q}$, (iii) $e^-q \to e^-qZ$, where in all processes the electron goes to beam pipeline. In the first process W^- decays leptonically and, if p_T^{miss} is sufficiently small, the process resembles the signal. In the second process if one of the jet fakes an electron it resembles the signal. In the third process Z decays leptonically and, if one of the leptons is missing, it resembles the signal too. These three background processes give much smaller contribution with respect to that of the main background processes (see Table 3).

The transverse momentum distribution of final state jets for signal at $\Lambda = 10$ TeV and for background is shown in Fig. 5. It is seen that $p_T > 150$ GeV cut essentially reduces background, whereas signal is almost unaffected. Figs. 6 and 7 represent pseudo-rapidity (η) distributions for electrons and jets, respectively. As seen from Fig. 7, η_{e^-} distribution for signal and background are not drastically different. Concerning η_j, most of signal lies above $\eta = 0$, whereas 99% of background is concentrated in $-2 < \eta_j < 0$ region. For this reasons below we use $p_T > 150$, $|\eta_e| < 4$ and $0 < \eta_j < 4$. With these cuts we present in Fig. 8 the invariant mass distributions for signal and background.

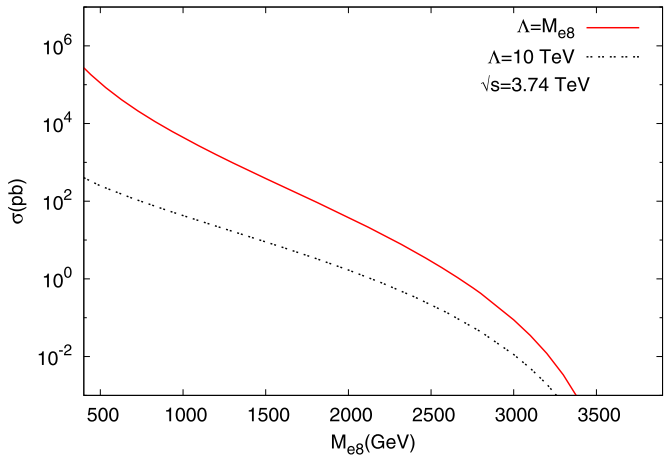

Fig. 4. Resonant e_8 production at the LHeC/EF.

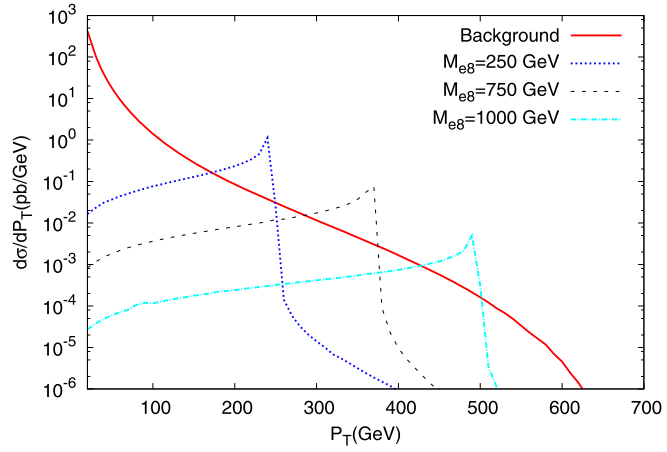

Fig. 5. Transverse momentum distributions of final state jets for signal and background at $\sqrt{s} = 1.4$ TeV and $\Lambda = 10$ TeV.

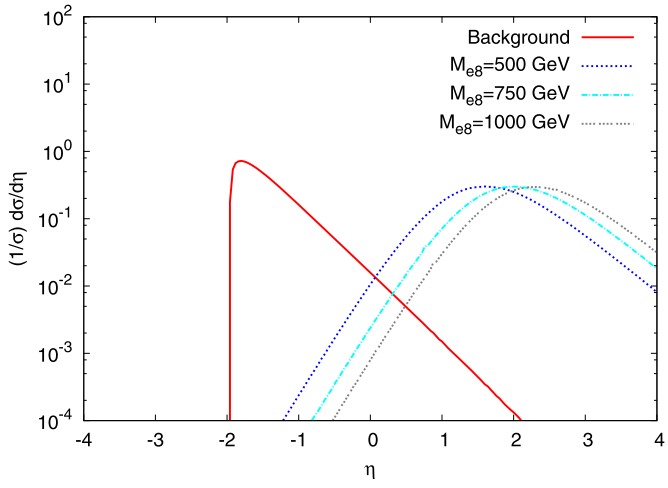

Fig. 6. Pseudo-rapidity distributions of jets for signal and background at $\sqrt{s} = 1.4$ TeV and $\Lambda = 10$ TeV.

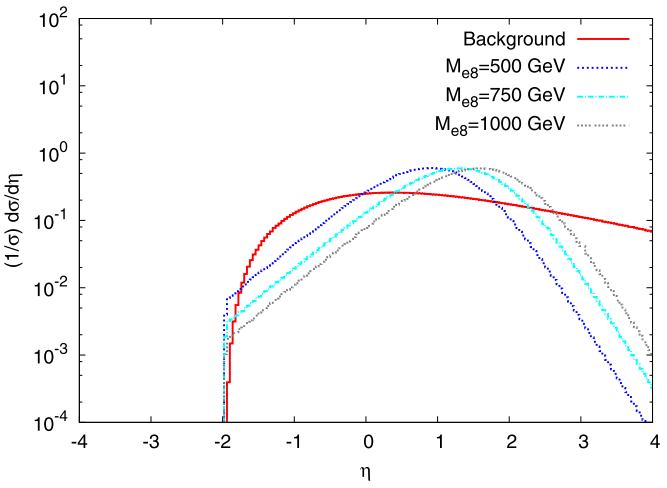

Fig. 7. Pseudo-rapidity distributions of electrons for signal and background at $\sqrt{s} = 1.4$ TeV and $\Lambda = 10$ TeV.

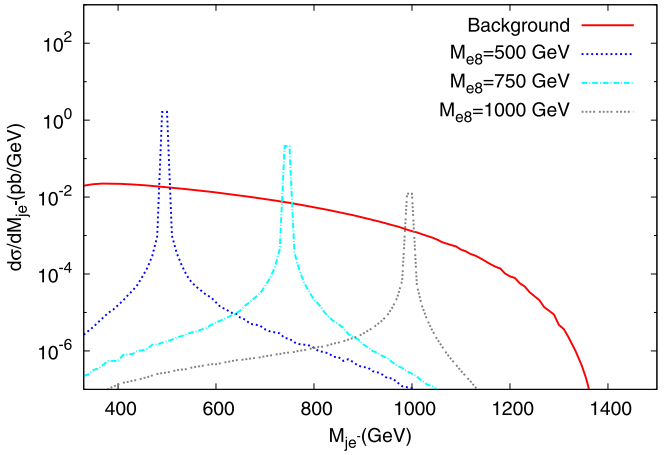

Fig. 8. ej invariant mass distributions for signal and background at $\sqrt{s} = 1.4$ TeV and $\Lambda = 10$ TeV.

Table 2
Number of signal and background events for LHeC/QCDE-1 with $L_{int} = 1$ fb^{-1}.

M_{e8}, GeV	$\Lambda = M_{e8}$		$\Lambda = 10$ TeV	
	S	B	S	B
500	1.1×10^7	1.1×10^3	3.3×10^4	700
750	6.4×10^5	630	4.2×10^3	280
1000	2.2×10^4	165	250	53
1250	81	6	1	1

The advantage of resonant production will provide an opportunity to probe compositeness scale will above the center of mass energy of the collider. For statistical significance we use following formula:

$$1\sigma = \frac{S}{\sqrt{S+B}} \tag{3}$$

where S and B denote number of signal and background events, respectively.

The number of signal and background events for different M_{e8} values are presented in Table 2 for $L_{int} = 1$ fb^{-1}. In calculating these values, in addition to cuts given above, we have used mass windows as $M_{e8} - 2\Gamma_{e8} < M_{ej} < M_{e8} + 2\Gamma_{e8}$ for $\Gamma_{e8} > 10$ GeV and $M_{e8} - 20$ GeV $< M_{ej} < M_{e8} + 20$ GeV for $\Gamma_{e8} < 10$ GeV. It is seen that the resonant production of the color octet electron

Table 3
Signal, major and minor background cross sections (in pb) for $M_{e8} = 1000$ GeV at LHeC/QCDE-1. For the processes $e^-g \to e^-q\bar{q}$ and $e^-q \to e^-qg$ we use jet ($\bar{q}, q$ or g) to electron fake rate 10^{-3}.

Subprocesses	$\Lambda = M_{e8}$ ($\Lambda = 10$ TeV)	
	$p_T^j > 150$ GeV	$p_T^{j,e^-} > 150$ GeV $M_{inv} = 1000 \pm 60$ (20) GeV
$e^-g \to e_8 \to e^-g$	27.4 (0.254)	21.7 (0.252)
$e^-q \to e^-q$	7.88	0.165 (0.0534)
$e^-q \to e^-W^-q \to e^-e^-\bar{\nu}_e q$	2.3×10^{-3}	4.5×10^{-6} (9.0×10^{-7})
$e^-g \to e^-q\bar{q}$	4.9×10^{-4}	1.84×10^{-8} (4.8×10^{-9})
$e^-q \to e^-qg$	0.118	2.46×10^{-7} (7.3×10^{-8})
$e^-q \to e^-Zq \to e^-e^-e^+q$	2.97×10^{-4}	2.96×10^{-7} (8.89×10^{-8})

Table 4
Achievable compositeness scale Λ in TeV units at LHeC/QCDE-1 for 5σ (3σ) statistical significance.

M_{e8}, GeV	$L_{int} = 1$ fb^{-1}	$L_{int} = 10$ fb^{-1}
500	150 (200)	275 (350)
750	65 (90)	125 (160)
1000	22 (30)	45 (58)

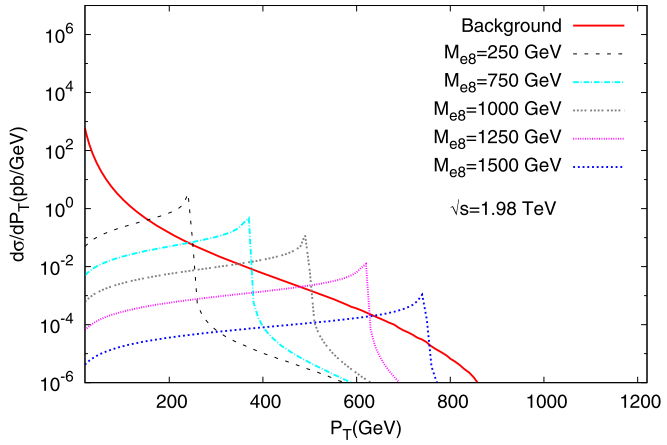

Fig. 9. Transverse momentum distributions of final state jets for signal and background at $\sqrt{s} = 1.98$ TeV and $\Lambda = 10$ TeV.

will provide very clean signature for masses up to $M_{e8} \simeq 1$ TeV. In Table 3 we give cross section values for signal, main and minor (mention above) background processes. It is seen that minor background processes have cross sections much smaller than that of major ones. In addition, requirement that primary electron goes to beam pipeline ($|\eta_e| > 4$) leads to further decrease of minor background processes cross sections by three order of magnitude. Moreover, contribution of the $e^-q \to e^-W^-q \to e^-e^-\bar{\nu}_e q$ process could be further suppressed using p_T^{miss} cut ($\backsim 0.3$ for $p_T^{miss} < 20$ GeV and $\backsim 0.1$ $p_T^{miss} < 10$ GeV). Concerning process $e^-q \to e^-Zq \to e^-e^-e^+q$ missing of positron leads to additional three order suppression.

The reachable compositeness scale values for $L_{int} = 1$ and $L_{int} = 10$ fb^{-1} are presented in Table 4. It is seen that multi-hundred TeV scale can be searched for $M_{e8} = 500$ GeV and the increase of the luminosity by one order gives two times higher values for Λ.

Lastly, for a given $L_{int} = 1$ fb^{-1}, the upper mass limits for 5σ discovery at LHeC/QCDE-1 stage are $M_{e8} = 1100$ GeV and $M_{e8} = 1275$ GeV for $\Lambda = 10$ TeV and $\Lambda = M_{e8}$, respectively.

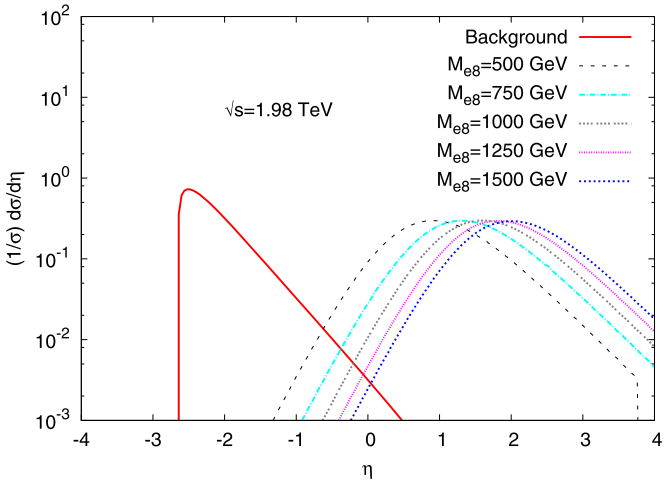

Fig. 10. Pseudo-rapidity distributions of jets for signal and background at $\sqrt{s} = 1.98$ TeV and $\Lambda = 10$ TeV.

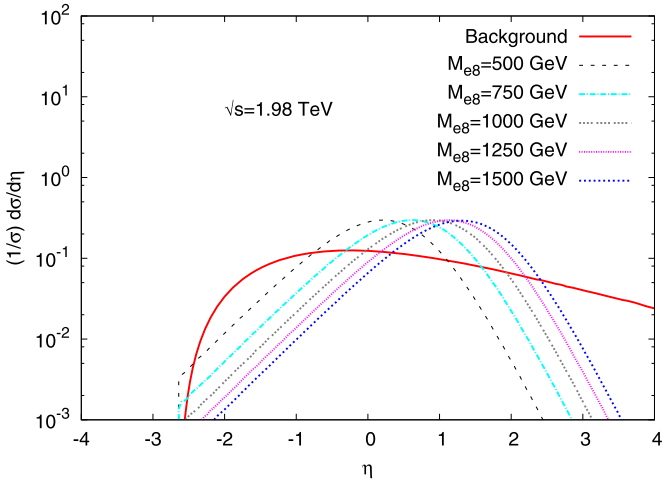

Fig. 11. Pseudo-rapidity distributions of electrons for signal and background at $\sqrt{s} = 1.98$ TeV and $\Lambda = 10$ TeV.

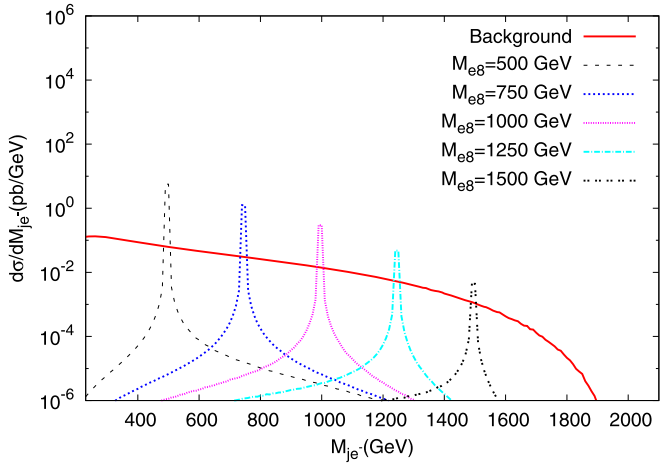

Fig. 12. ej invariant mass distributions for signal and background at $\sqrt{s} = 1.98$ TeV and $\Lambda = 10$ TeV.

Table 5
Number of signal and background events for LHeC/QCDE-2 with $L_{int} = 1$ fb^{-1}.

M_{e8}, GeV	$\Lambda = M_{e8}$		$\Lambda = 10$ TeV	
	S	B	S	B
500	3.3×10^7	1.4×10^3	9.8×10^4	940
750	3.9×10^6	1000	2.6×10^4	445
1000	5.0×10^5	630	5.8×10^3	210
1250	5.3×10^4	270	980	76
1500	3.5×10^3	77	89	16
1750	55	6	2	1

Table 6
Achievable compositeness scale Λ in TeV units at LHeC/QCDE-2 for 5σ (3σ) statistical significance.

M_{e8}, GeV	$L_{int} = 1$ fb^{-1}	$L_{int} = 10$ fb^{-1}
500	245 (320)	440 (570)
750	150 (195)	275 (355)
1000	82 (110)	155 (205)
1250	41 (56)	81 (107)
1500	16 (23)	34 (46)

3.2. LHeC/QCDE-2 stage

In order to determine the corresponding cuts we present p_T, η_j and η_e distributions for signal and background processes in Figs 9, 10 and 11, respectively. The figures indicate that significant change takes place only for η_j. In this subsections we will use $p_T > 150$, $|\eta_e| < 4$ and $-0.5 < \eta_j < 4$. The invariant mass distributions obtained with this cuts are given in Fig. 12.

The numbers of signal and background events for 6 different M_{e8} values are presented in Table 5 (the mass window used is the same as the one used in previous subsection). As seen from the table very clean signal can be obtained up to $M_{e8} \backsimeq 1500$ GeV.

The reachable Λ scales for 5 different mass values are given in Table 6. Comparison with Table 4 shows that twofold increasing of the electron energy results in: 1.5 times higher values of Λ for $M_{e8} = 500$ GeV, 2 times – for $M_{e8} = 750$ GeV and 4 times – for $M_{e8} = 1000$ GeV. Moreover, multi-ten TeV scales can be achieved for $M_{e8} = 1250$ and 1500 GeV, which are not available at LHeC/QCDE-1.

Finally, for a given $L_{int} = 1$ fb^{-1}, the upper mass limits for 5σ discovery at LHeC/QCDE-2 are $M_{e8} = 1580$ GeV and $M_{e8} = 1775$ GeV for $\Lambda = 10$ TeV and $\Lambda = M_{e8}$, respectively.

4. Conclusion

It seems that QCD Explorer stage(s) of the LHeC, together with providing necessary information on PDF's and QCD basics, could play essential role on the BSM physics, also. Concerning color octet electrons. LHeC/QCDE-1 will cover M_{e8} mass up to O(1200 GeV), whereas LHeC/QCDE-2 will enlarge covered mass range up to O(1700 GeV).

The discovery of e_8 at this machine, simultaneously will determine compositeness scale. For example if $M_{e8} = 500$ GeV, LHeC/QCDE-2 with $L_{int} = 10$ fb^{-1} will be sensitive to Λ up to 570 TeV.

Acknowledgements

Authors are grateful to A. Celikel and M. Kantar for useful discussions. This work is supported by TUBITAK in the framework of post-doctoral program and TAEK under the grant No. CERN-A5.H2.P1.01-11.

References

[1] I.A. D' Souza, C.S. Kalman, PREONS: Models of Leptons, Quarks and Gauge Bosons as Composite Objects, World Scientific Publishing Co., 1992.
[2] H. Harari, Phys. Lett. B 86 (1979) 83.
[3] H. Fritzch, G. Mandelbaum, Phys. Lett. B 102 (1981) 319.
[4] O.W. Greenberg, J. Sucher, Phys. Lett. B 99 (1981) 339.
[5] R. Barbieri, R.N. Mohapatra, A. Maseiro, Phys. Lett. B 105 (1981) 369.
[6] U. Baur, K.H. Streng, Phys. Lett. B 162 (1985) 387.
[7] A. Celikel, M. Kantar, S. Sultansoy, Phys. Lett. B 443 (1998) 359.
[8] G. Amsler, et al., Particle Data Group, Phys. Lett. B 667 (2008) 1.
[9] F. Abe, et al., Phys. Rev. Lett. 63 (1989) 1447.
[10] J.L. Hewett, T.G. Rizzo, Phys. Rev. D 56 (1997) 9.
[11] I. Abt, et al., Nucl. Phys. B 396 (1993) 3;
T. Ahmed, et al., Z. Phys. C 64 (1994) 545.
[12] S. Sultansoy, Eur. Phys. J. C 33 (2004) S1064.
[13] S. Sultansoy, in: Proceedings of Particle Accelerator Conference, Knoxville, 2005, p. 4329.
[14] A.N. Akay, H. Karadeniz, S. Sultansoy, arXiv:0911.3314 [physics.acc-ph].
[15] The LHeC web page, http://www.lhec.org.uk.
[16] J.B. Dainton, et al., JINST 1 (2006) P10001.
[17] D. Schulte, F. Zimmerman, in: Proceedings of European Particle Accelerator Conference, Lucerne, Switzerland, 2004, p. 632.
[18] H. Karadeniz, S. Sultansoy, in: Proceedings of European Particle Accelerator Conference, Edinburgh, 2006, p. 673.
[19] F. Zimmermann, et al. in: Proceedings of European Particle Accelerator Conference, Genoa, Italy, 2008, p. 2847.
[20] A. Celikel, M. Kantar, Tr. J. Phys. 22 (1998) 401.
[21] A. Pukhov, et al., hep-ph/9908288.
[22] D. Stump, et al., JHEP 0310 (2003) 046.